Opt Quant Electron (2016) 48:47
DOI 10.1007/s11082-015-0296-x

Influence of cavity parameters on pulse properties of dual wavelength Yb:YAG mode-locked laser

Jieyu Wang[1] · Li Wang[1] · Yi Zhan[1]

Received: 1 April 2015 / Accepted: 19 September 2015 / Published online: 19 December 2015

Abstract A theoretical study on the influence of cavity parameters on pulse properties of dual wavelength Yb:YAG mode-locked laser has been carried out. Using coupled rate-equations, the relations of the small signal gain to the cavity parameters are simulated at first. The calculation results are taken into Haus's master equation to investigate the effects of cavity parameters on the properties of dual-wavelength mode-locking pulses. The results show that, increasing the cavity length, output coupling rate and beam radius in the laser crystal in a proper regime is benefit for pulse energies enhancement, and the pulse widths will be broadened very little.

Keywords Dual wavelength lasers · Mode locking · Small signal gain · Pulse energy · Pulse width

1 Introduction

Ultrafast solid-state lasers have become the key enabling technology in science and industry fields, with applications including ultrafast spectroscopy, metrology, superfine material processing and microscopy (Südmeyer et al. 2008; Keller 2010; Shah et al. 2006). Among those, dual-wavelength mode-locked lasers are attractive sources for generating ultrahigh repetition rate pulse trains. Furthermore, by difference-frequency mixing in nonlinear crystals, they can also generate ultrashort pulses in the infrared region. Some demonstrations of dual-wavelength mode locking based on a single or double cavity were published, including Ti:sapphire lasers (Zhu et al. 2005; Zhang and Yagi 1993) and rare-

✉ Li Wang
lwang.1@bjut.edu.cn

Jieyu Wang
solomngg@163.com

[1] College of Applied Sciences, Beijing University of Technology, Beijing 100124, China

earth doped solid state lasers (Cong et al. 2011; Xu et al. 2012; Yang et al. 2012; Yoshioka et al. 2009, 2010; Zhuang et al. 2013).

Among solid-state laser materials, Yb:YAG crystal is a promising material for generating high pulse energy, ultrashort laser pulses (Saraceno et al. 2012, 2014; Brons et al. 2014). Its wide absorption band at 940 nm allows for the directly laser-diode pumping, and broad emission spectrum is benefit for femtosecond pulse generation. The small quantum defect, high quantum efficiency and low thermal loading enable a highly efficient operation. Moreover, transitions from the energy level $^2F_{5/2}$–$^2F_{7/2}$ of Yb:YAG lead to laser operation at two main peaks located around 1030 and 1050 nm under optical excitation at 940 nm. Thus the Yb:YAG crystal has a capability of generating dual-wavelength ultrashort pulses and a demonstration is reported very recently (Zhuang et al. 2013).

To understand the dynamics of dual-wavelength mode-locked lasers, the rate equations are efficient tool to simulate the forming process of dual-wavelength lasers. Several theoretical research were carried out for different laser materials, including Ti:sapphire (Song et al. 2001), Nd:YAG (Henderson 1990; Sato et al. 2014) and Nd:$YAlO_3$ (Lin et al. 2003). Nevertheless, the studies were focus on the Q-switching behavior, while the analysis of mode-locking operation has not been reported. Moreover, it should be noted that the stimulated-emission cross section of 1030 nm emission is much larger than that of 1050 nm emission. The output coupling and cavity length of the 1030 nm laser set to be larger and shorter than those for 1050 nm is an common and efficient way to compensate for the difference in the stimulated-emission cross section between the two laser transitions. Therefore, to study the influence of cavity parameters on pulse properties is meaningful to achieve the dual wavelength mode-locking operation. In this paper, we investigate the effects of cavity parameters, such as cavity length, output coupling rate and beam radius in the laser crystal, on dual-wavelength mode-locking pulses generation in a solid-state Yb:YAG laser. By using a rate-equation model, numerical simulations are performed at first to investigate the relations of small signal gain to the cavity parameters. Based on this, the influence of cavity parameters on properties of dual-wavelength mode-locking pulses are studied by using Haus's master equation. The numerical results presented here may be benefit for choosing suitable values to improve the dual-wavelength mode-locking performance in a solid-state laser.

2 Small signal gain calculation

We assumed a Y-shaped cavity was considered in our numerical model (Henderson 1990; Sato et al. 2014). In this configuration, an output mirror and a Yb:YAG laser crystal are shared between two lasers, and a saturable absorber and a rear mirror for each laser are placed in the respective arms of the laser cavities. The coupled rate equations are applied to describe the dual-wavelength oscillations, which is similar to Henderson's numerical model (Henderson 1990):

$$\frac{dN}{dt} = W_p(t) - \frac{N}{\tau_f} - Nc\left(\sigma_1\phi_1\frac{L}{L_1} + \sigma_2\phi_2\frac{L}{L_2}\right) \tag{1}$$

$$\frac{d\phi_1}{dt} = c\sigma_1 N\phi_1\frac{L}{L_1} - \frac{\phi_1}{\tau_{p_1}} + \frac{N\gamma_1\beta_1}{\tau_f} \tag{2}$$

$$\frac{d\phi_2}{dt} = c\sigma_2 N\phi_2 \frac{L}{L_2} - \frac{\phi_2}{\tau_{p_2}} + \frac{N\gamma_2\beta_2}{\tau_f} \tag{3}$$

where $N(t)$ is the inverted population density in the upper laser manifold, $\phi_1(t)$ and $\phi_2(t)$ are the photon densities for two laser transitions in the cavities, τ_f is the lifetime of the upper laser manifold, σ_1 and σ_2 are the stimulated-emission cross sections for two transitions, L is the laser crystal length, L_1 and L_2 are the effective lengths of the cavities, c is the speed of light in vacuum, γ_1 and γ_2 are the rates at which spontaneous emission contributes to the lasers, β_1 and β_2 are the luminescence branching ratios for the two transitions. The pumping rate $W_p(t)$ can be written as follows by taking the initial population density into account:

$$W_p(t) = \frac{P_{pump}}{N_0 h v_p V}[N_0 - N(t)] \tag{4}$$

where P_{pump} is the pump power, h is Planck's constant, v_p is the angular frequency of pump wavelength at 940 nm, V is the effective laser medium volume. The photon lifetimes in the laser cavities τ_{p_1} and τ_{p_2} are given by:

$$\tau_{p_1} = -\frac{2L_1}{c\ln[(1-\alpha)(1-T_1)]} \tag{5}$$

$$\tau_{p_2} = -\frac{2L_2}{c\ln[(1-\alpha)(1-T_2)]} \tag{6}$$

where α is the round trip loss, T_1 and T_2 are the output coupling rates. The subscripts 1 and 2 in the equations correspond to the laser transitions at 1030 and 1050 nm, respectively.

To calculate the small signal gain of each laser transition in the laser cavities, we used a fourth-order Runge–Kutta program to solve the coupled rate equations. The inverted population density in the steady regime should be derived at first. Using this inverted population density, we calculate the photon density ϕ after one round trip time with a relative small initial photon density ϕ_0 and then compare them to obtain the small signal gain (Balembois et al. 1997):

$$G = I_i/I_{i0} = \phi_i/\phi_{i0}, i = 1, 2 \tag{7}$$

where G is small signal gain, I_{i0} is initial laser power density and I_i is the power density

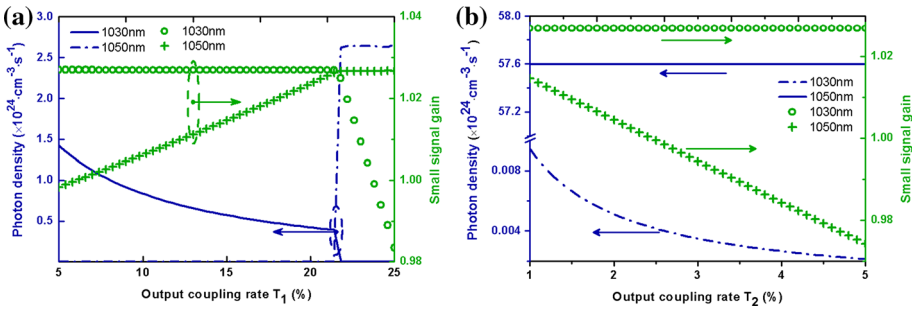

Fig. 1 Photon densities and small signal gains of two wavelengths versus output coupling rates of **a** 1030 nm laser and **b** 1050 nm laser

after one round trip. The subscript i refers to two separate laser transitions at 1030 and 1050 nm. The parameters used in the simulation are given as follows. The pump power P_{pump} is 30 W with the spot size of 100 μm in the laser crystal. The cavity length L_1 and L_2 are both 5 m and the crystal length L is 1 mm. The transmittances of output mirror are $T_1 = 15$ % and $T_2 = 1$ %. The round trip loss α is 3 %. The parameters of Yb:YAG laser crystal are taken from previous researches (Hönninger et al. 1999a, b; Brown and Vitali 2011): the stimulated-emission cross sections for two transitions are $\sigma_1 = 2.1 \times 10^{20}$ cm^2 and $\sigma_2 = 2.1 \times 10^{20}$ cm^2, the fluorescence lifetime $\tau_f = 0.95$ ms, the fluorescence branching ratios are $\beta_1 = 0.342$ and $\beta_2 = 0.088$. The quantities γ_1 and γ_2 can be roughly estimated because the last terms in Eqs. (2) and (3) are important in determining the initial photon density, but can be omitted after the oscillations start.

The relations of photon densities and small signal gain to the output coupler rates T_1 and T_2 are illustrated in Fig. 1. One of output coupler rates is fixed when another changes. The oscillation threshold of small signal gain is 1, because the round-trip gain has to be equal to the round-trip losses in order to achieve laser oscillation. Otherwise, the laser will not be amplified in the cavity. As shown in Fig. 1a, there exist a critical value of output coupling rate T_1, at which the photon density and small signal gain of two lasers are equal, respectively. Before T_1 reach this value, the small signal gain of 1050 nm laser starts from the threshold and increases as T_1 becomes larger, while the one of 1030 nm laser almost keeps constant. The photon density of 1030 nm laser decreases gradually but still larger than that of 1050 nm laser. After that, however, the small signal gain of 1030 nm laser drops quickly, while that of 1050 nm laser become stable. And the photon density of 1050 nm laser increases sharply, while that of 1030 nm laser decreases very fast and then the oscillation cease. In Fig. 1b, we could see that when T_2 increase, the photon density and small signal gain of 1050 nm decrease rapidly, while those of 1030 nm laser are not changed with the variation. The simulation results indicate that the photon densities and small signal gain are sensitive to output coupling rates. If the transmittance for one wavelength gets too large, the corresponding oscillation will soon cease the operation. Therefore, the output mirror should be designed and coated precisely in order to achieve the dual wavelength operation, and the pump threshold also could be reduced.

The relations of photon densities and small signal gain to the cavity length L_1 and L_2 are illustrated in Fig. 2. One of the cavity length is fixed when another changes. As can be seen, when the cavity length related to one wavelength gets longer, the photon density and small signal gain of the corresponding wavelength are both increase. Moreover, the photon density and small signal gain of another wavelength will not be affected by this variation,

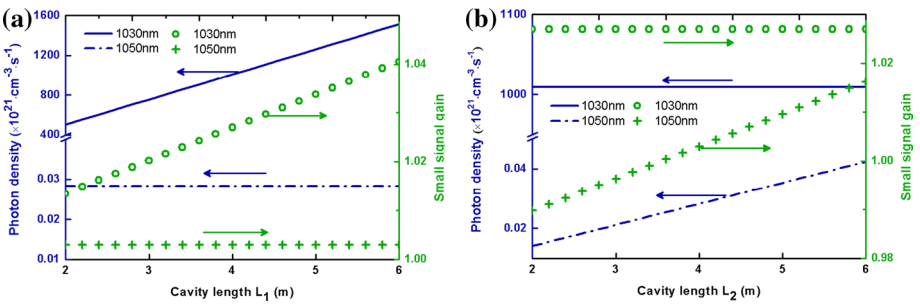

Fig. 2 Photon densities and small signal gains of two wavelengths versus cavity lengths of **a** 1030 nm laser and **b** 1050 nm laser

indicating that to make the cavity length for one wavelength longer is an effective way to increase the intracavity power of the corresponding laser, while the power of another laser will not be reduced as the price. The relation of photon densities and small signal gain to the beam radius in the laser crystal is illustrated in Fig. 3. As shown in Fig. 3, when the beam radius becomes larger, the photon density of 1030 nm laser decrease, and other parameters are almost independent to this variation. It implies that it is better to make the beam radius smaller, so that the intracavity power of two lasers can be increased.

3 Pulse properties of dual-wavelength mode-locked laser

To study the pulse properties of dual-wavelength mode-locked laser, the stable mode-locking threshold condition should also be considered. Hönninger et al. (1999a, b) give the stable mode-locking condition against Q-switching mode-locking:

$$E_{P,c} = (F_{sat,L}A_{eff,L}F_{sat,A}A_{eff,A}\Delta R)^{1/2} \tag{8}$$

where $E_{P,c}$ is critical intracavity pulse energy, $F_{sat,L}$ is the saturation fluence of the gain medium, $A_{eff,L}$ is the effective laser mode area inside the gain medium, $F_{sat,A}$ is the saturation energy of saturable absorber and ΔR is the modulation depth. We focus on the influence of $F_{sat,L}$ and $A_{eff,L}$ on the pulse properties in this paper. The intracavity pulse energy can be calculated by Haus's master equation reads as follows (Haus 1975; Kartner et al.1996)

$$T_R\frac{\partial}{\partial T}A(T,t) = \left[-iD\frac{\partial^2}{\partial t^2} + i\delta|A|^2\right]A + \left[g - L_{loss} + D_{g,f}\frac{\partial^2}{\partial t^2} - q(T,t)\right]A \tag{9}$$

where $A(T, t)$ is slowly varying field envelope, D is the intracavity GDD, $\delta = (2\pi n_2/\lambda_l A_l)l$ is SPM coefficient, n_2 is intensity dependent refractive index of the laser crystal, L_{loss} is round-trip loss, $D_{g,f} = g/\Omega_g^2 + 1/\Omega_f^2$ is the gain and intracavity filter dispersion, Ω_g and Ω_f are the HWHM gain and filter bandwidth, respectively. The saturated gain g is defined as

$$g(T) = \frac{g_0}{1 + \frac{E_p(T)}{P_L T_R}} \tag{10}$$

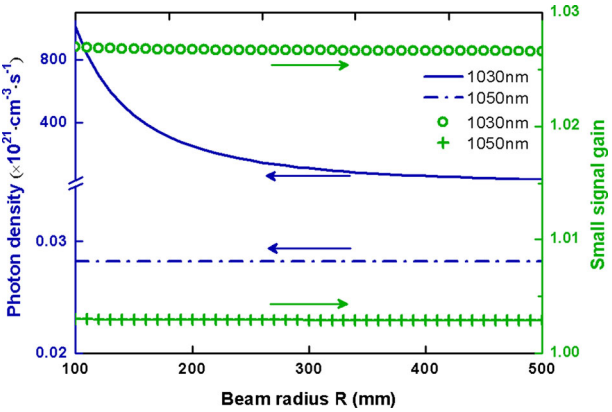

Fig. 3 Photon density and small signal gain of two lasers versus beam radius in the laser crystal

where g_0 is small signal gain, $E_p(T) = \int_{-\infty}^{\infty} |A(T)|^2 dt$ is pulse energy, P_L is the saturation power of laser crystal. If the recovery time of the saturable absorber is comparable or even longer than the final pulse width, the absorber is assumed to saturate according to the following

$$\frac{\partial q(T,t)}{\partial t} = \frac{q - q_0}{\tau_A} - \frac{|A(T,t)|^2}{E_A} q \tag{11}$$

where $q_0 = \Delta R$ is the initial saturable absorption, τ_A is the relaxation time and E_A the saturation energy of the absorber. However, if the pulse is much longer than the relaxation time, the absorber dynamics is described by

$$q(T,t) = \frac{q_0}{1 + \frac{|A(T,t)|^2}{P_A}} \text{with } P_A = \frac{E_A}{\tau_A} \tag{12}$$

where P_A is the saturation power of the saturable absorber.

The master equation can be solved by using split-step Fourier method. The parameters used in the simulation are set to be: $n_2 = 6.9 \times 10^{-20}$ m^2/W, $\Delta R = q_0 = 1$ %, $F_{sat,a} = 90$ μJ/cm^2, $\tau_A = 0.5$ ps and $T_1 = 5$ %, $F_{sat,l}$ is 4.6 J/cm^2 for 1030 nm and 30 J/cm^2 for 1050 nm, Ω_g is 1.78THz for 1030 nm and 1.58THz for 1050 nm, other parameters are the same as for Sect. 2. For simplicity, we consider the simultaneous dual-wavelength mode-locking, i.e., the cavity length L_1 is equal to L_2. As discussed in Sect. 2, the oscillation threshold will be reduced by increasing the cavity length. Therefore, the threshold of output coupling rate T_1 for dual-wavelength performance will become lower with increasing cavity length when T_2 is fixed. Assuming T_2 is 1 %, taking the corresponding values of T_1 and cavity length into Eq. (9), and considering the stable mode-locking condition Eq. (8), the relation of intracavity pulse energy to the cavity length is illustrated in Fig. 4. As can be seen, the pulse energies of two oscillations both become higher when the cavity length gets longer, because the small signal gains of two wavelengths are proportional to the cavity length, and the smaller output coupling rate T_1 make the 1030 nm laser pulses suffer less round trip loss. It should be noted that further cavity length

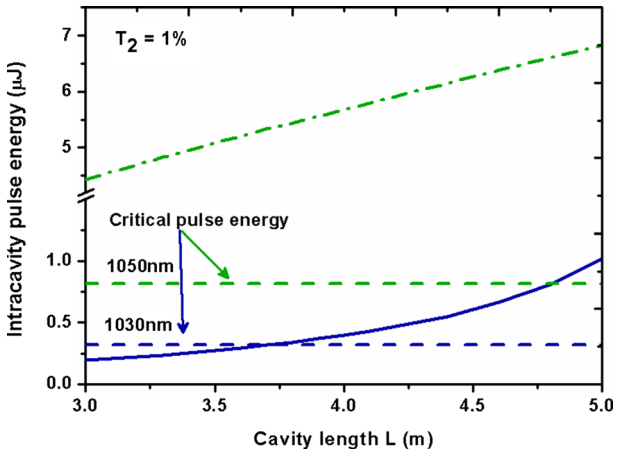

Fig. 4 Intracavity pulse energy versus cavity length for two wavelength

increase will make the pulse energy of 1050 nm laser too much higher than the saturation fluence of saturable absorber, leading to unstable pulses. However, if the cavity length is shorter than 3.75 m, the pulse energy of 1030 nm laser is smaller than the stable mode-locking threshold, indicating that the dual-wavelength mode-locking will not occur, and stable mode-locking achievement is a bit easier for the wavelength of 1050 nm than for 1030 nm when laser is in a performance of dual wavelength oscillation, which is in agreement with the experimental results (Yoshioka et al. 2009, 2010). The reason of this phenomenon is that the threshold T_1 of shorter length cavity is still too high, and the 1030 nm laser pulses suffer too much loss per round trip and can't reach the stable mode-locking threshold.

The relations of the output pulse energy and pulse width to the output coupler rate T_1 are illustrated in Fig. 5. As shown in Fig. 5, when T_1 becomes higher, the pulse energy of 1030 and 1050 nm laser pulses both increase, whereas the pulse width of 1030 nm laser become

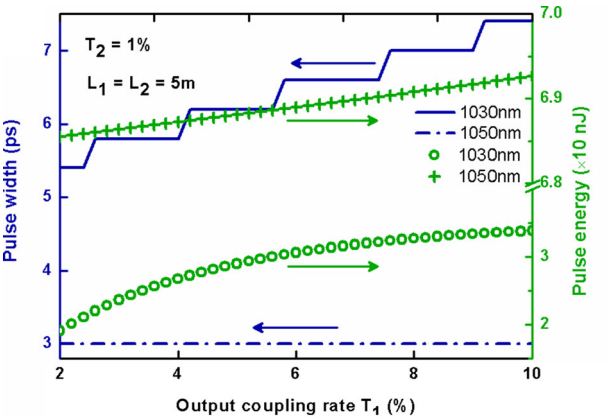

Fig. 5 Output pulse energies and pulse widths of two wavelengths versus cavity length output coupling rate of 1030 nm laser

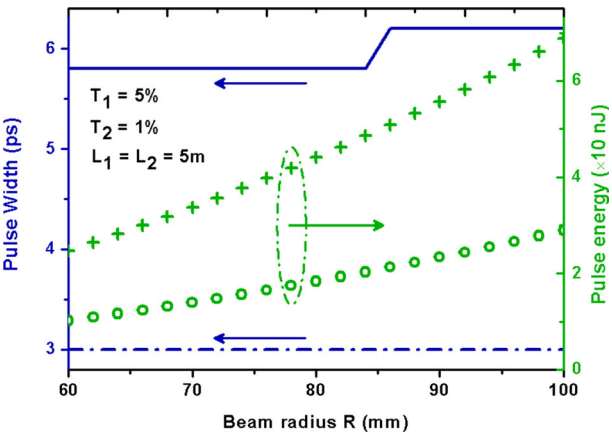

Fig. 6 Output pulse energies and pulse widths of two wavelengths versus beam radius in the laser crystal

wide gradually while that of 1050 nm laser is unchanged. That can be understood that the small signal gain of 1050 nm laser increase with a growing up T_1 when T_2 is fixed, thus the pulse energy of 1050 nm laser grows up with unchanged pulse width. The small signal gain of 1030 nm laser almost keeps constant when T_1 increase, so higher T_1 is favorable for intracavity pulse energy coupling out, although the increasing T_1 make the pulse width grow wider a little. Note that, the intracavity pulse energy decrease when T_1 increase, indicating that T_1 can't be too high, or the 1030 nm laser can't operate in the stable mode-locking regime. The relations of the output pulse energy and pulse width to the beam radius in the laser crystal are illustrated in Fig. 6. As shown in Fig. 6, the pulse energies of two wavelengths both become higher as beam radius become larger, while the pulse widths change very little. According to Eq. (10), we know that the saturation power of laser crystal P_L becomes bigger as the beam radius gets larger. Nevertheless, the variations of small signal gain of two wavelengths are very little. Therefore, the pulses will travel more round trips to reach the saturated gain if the beam radius is larger, indicating that the pulses energies will be promoted efficiently, compare to those in the smaller beam radius condition.

4 Conclusion

In conclusion, We have investigated the influence of cavity parameters, such as cavity length, output coupling rate and beam radius in the laser crystal, on pulse properties in dual-wavelength Yb:YAG mode-locked lasers. Numerical simulations of the relations of the small signal gain of each wavelength to the cavity parameters are performed at first by using a rate-equation model. Taking the calculation results into Haus's master equation, the effects of cavity parameters on the properties of dual-wavelength mode-locking pulses are discussed theoretically. The results show that, increasing the cavity length, output coupling rate and beam radius in the laser crystal in a proper regime is benefit for pulse energies enhancement, and the pulse widths will be broadened very little. However, if the chosen value is too big or small, the pulses of one wavelength will not be stable, and dual-wavelength mode-locking can't be achieved.

Acknowledgments This work was supported by the Key Project of Beijing Municipal Education Commission Research Program (Kz201110005010) and special programs for advanced talents of the sea poly project.

References

Balembois, F., Falcoz, F., Kerboull, F., Druon, F., Georges, P., Brun, A.: Theoretical and experimental investigations of small-signal gain for a diode-pumped Q-switched Cr:LiSAF laser. IEEE J. Quantum Electron. **33**, 269–278 (1997)

Brons, J., Pervak, V., Fedulova, E., Bauer, D., Sutter, D., Kalashnikov, V., Apolonskiy, A., Pronin, O., Krausz, F.: Energy scaling of Kerr-lens mode-locked thin-disk oscillators. Opt. Lett. **39**, 6442–6445 (2014)

Brown, D.C., Vitali, V.A.: Yb:YAG kinetics model including saturation and power conservation. IEEE J. Quantum Electron. **47**, 3–12 (2011)

Cong, Z., Tang, D., Tan, W., Zhang, J., Xu, C., Luo, D., Xu, X., Li, D., Xu, J., Zhang, X., Wang, Q.: Dual-wavelength passively mode-locked Nd:LuYSiO5 laser with SESAM. Opt. Express **19**, 3984–3989 (2011)

Haus, H.A.: Theory of mode-locking with a fast saturable absorber. J. Appl. Phys. **46**, 3049–3058 (1975)

Henderson, G.A.: A computational model of a dualwavelength solidstate laser. J. Appl. Phys. **68**, 5451 (1990)

Hönninger, C., Paschotta, R., Graf, M., Morier-Genoud, F., Zhang, G., Moser, M., Biswal, S., Nees, J., Braun, A., Mourou, G.A., Johannsen, I., Giesen, A., Seeber, W., Keller, U.: Ultrafast ytterbium-doped bulk lasers and laser amplifiers. Appl. Phys. B **69**, 3–17 (1999a)

Hönninger, C., Paschotta, R., Morier-Genoud, F., Moser, M., Keller, U.: Q-switching stability limits of continuous-wave passive mode locking. J. Opt. Soc. Am. B **16**, 46–56 (1999b)

Kartner, F.X., Jung, I.D., Keller, U.: Soliton mode-locking with saturable absorber. IEEE J. Sel. Top. Quantum Electron. **2**, 540–556 (1996)

Keller, U.: Femtosecond to attosecond optics. IEEE Photonics J. **2**, 3 (2010)

Lin, W., Lin, S., Huang, J.: Cavity configuration for a Q-switched simultaneous dual-wavelength Nd:YAlO3 laser with the characteristic of polarization-dependent emission cross section. J. Opt. Soc. Am. B **20**, 479–483 (2003)

Saraceno, C.J., Emaury, F., Heckl, O.H., Baer, C.R.E., Hoffmann, M., Schriber, C., Golling, M., Sudmeyer, T., Keller, U.: 275 W average output power from a femtosecond thin disk oscillator operated in a vacuum environment. Opt. Express **20**, 23535–23541 (2012)

Saraceno, C.J., Emaury, F., Schriber, C., Hoffmann, M., Golling, M., Südmeyer, T., Keller, U.: Ultrafast thin-disk laser with 80 μJ pulse energy and 242 W of average power. Opt. Lett. **39**, 9–12 (2014)

Sato, A., Okubo, S., Asai, K., Ishii, S., Mizutani, K.: Energy extraction in dual-wavelength Q-switched laser with a common upper laser level. Appl. Phys. B **117**, 621–631 (2014)

Shah, L., Fermann, M.E., Dawson, J.W., Barty, C.P.J.: Micromachining with a 50 W, 50 μJ, subpicosecond fiber laser system. Opt. Express **14**, 12546–12551 (2006)

Song, F., Yao, J.Q., Zhou, D.W., Qiao, J.Y., Zhang, G.Y., Tian, J.G.: Rate-equation theory and experimental research on dual-wavelength operation of a Ti:sapphire laser. Appl. Phys. B **72**, 605–610 (2001)

Südmeyer, T., Marchese, S.V., Hashimoto, S., Baer, C.R.E., Gingras, G., Witzel, B., Keller, U.: Femtosecond laser oscillators for high-field science. Nat. Photonics **2**, 599–604 (2008)

Xu, J.L., Guo, S.Y., He, J.L., Zhang, B.Y., Yang, Y., Yang, H., Liu, S.D.: Dual-wavelength asynchronous and synchronous mode-locking operation by a Nd:CLTGG disordered crystal. Appl. Phys. B. **107**, 53–58 (2012)

Yang, Q., Wang, Y.G., Liu, D.H., Liu, J., Zheng, L.H., Su, L.B., Xu, J.: Dual-wavelength mode-locked Yb:LuYSiO5 laser with a double-walled carbon nanotube saturable absorber. Laser Phys. Lett. **9**, 135–140 (2012)

Yoshioka, H., Nakamura, S., Ogawa, T., Wada, S.: Diode-pumped mode-locked Yb:YAG ceramic laser. Opt. Express **17**(11), 8919–8925 (2009)

Yoshioka, H., Nakamura, S., Ogawa, T., Wada, S.: Dual-wavelength mode-locked Yb:YAG ceramic laser in single cavity. Opt. Express **18**, 1479–1486 (2010)

Zhang, Z., Yagi, T.: Dual-wavelength synchronous operation of a mode-locked Ti:sapphire laser based on self-spectrum splitting. Opt. Lett. **18**, 2126–2128 (1993)

Zhu, C.J., He, J.F., Wang, S.C.: Generation of synchronized femtosecond and picosecond pulses in a dual-wavelength femtosecond Ti:sapphire laser. Opt. Lett. **30**, 561–563 (2005)

Zhuang, W.Z., Chang, M.T., Su, K.W., Huang, K.F., Chen, Y.F.: High-power terahertz optical pulse generation with a dual-wavelength harmonically mode-locked Yb:YAG laser. Laser Phys. **23**, 075803 (2013)